Journal of Engineering and Applied Sciences 13 (6): 1575-1583, 2018
ISSN: 1816-949X


# Development of Hybrid Computational Intelligence Model for Estimating Relative Cooling Power of Manganite-Based Materials for Magnetic Refrigeration Enhancement

[1]Nahier Aldhafferi, [2, 3]Taoreed O. Owolabi, [4]Kabiru O. Akande,
[5]Sunday O. Olatunji and [1]Abdullah Alqahtani
[1]Department of Computer Information System,
College of Computer Science and Information Technology,
University of Dammam, Dammam, Kingdom of Saudi Arabia
[2]Department of Physics, King Fahd University of Petroleum and Minerals,
Dhahran, Kingdom of Saudi Arabia
[3]Department of Physics and Electronics, Adekunle Ajasin University,
Akungba Akoko, Ondo State, Nigeria
[4]Institute for Digital Communications, School of Engineering,
University of Edinburgh, Edinburgh, United Kingdom
[5]Department of Computer Science, College of Computer Science and Information Technology,
University of Dammam, Dammam, Kingdom of Saudi Arabia

**Abstract:** The significance of Relative Cooling Power (RCP) of manganite-based magnetic refrigerant in Magnetic Refrigeration (MR) technology cannot be over-emphasized. Although, MR system overcomes the setbacks of conventional gas compression technology with its better performance, low cost and little or no environmental hazard. However, experimental determination of the refrigerant RCP is subjected to procedures and routines that are not only challenging but also consume appreciable time and other valuable resources. This necessitates for a simple and cost effective modeling technique that preserves the experimental precision and accuracy. Therefore, this research develops Sensitivity-Based Linear Learning Method (SBLLM) of training two-layer feedforward neural network for estimating RCP of manganite-based materials using ionic radii and dopants concentration as inputs to the model. The number of epoch and hidden neurons of the network are optimized using Gravitational Search Algorithm (GSA). The results of the developed GSA-SBLLM Model agree well with the experimentally measured values. The strength and robustness of the developed GSA-SBLLM Model include its ability to incorporate up to four different dopants and their respective concentrations to manganite material for magnetic refrigerant RCP estimation. This ability coupled with the precision of its estimates is of significant impact in magnetic refrigeration enhancement without experimental challenges.

**Key words:** Manganite-based materials, relative cooling power, sensitivity-based linear learning method, ionic radii, gravitational search algorithm, magnetic refrigeration

## INTRODUCTION

The potentials of Magnetic Refrigeration (MR) as emerging cooling technology in energy consumption and preventing climate catastrophes around the globe cannot be overemphasized (Bruck, 2005; Gschneidner *et al*., 2005). Besides being an efficient cooling technology, its low cost and low noise operational features significantly contribute to its preference over the conventional gas compression cooling system and make it a better choice in cooling industry as well as other industries where refrigeration is paramount. Magnetocaloric effect of manganite-based refrigerant which arises from isothermal change in entropy or adiabatic change in temperature due to externally applied magnetic field is the main factor responsible for the cooling effect of MR technology (Messaoui *et al*., 2017; Taran *et al*., 2015; Bettaibi *et al*., 2015; Selmi *et al*., 2015; Gdaiem *et al*., 2016; Owolabi *et al*., 2016). Magnetocaloric effect occurs due to the presence of phonon and magnon excitations which are coupled by

**Corresponding Author:** Taoreed O. Owolabi, Department of Physics, King Fahd University of Petroleum and Minerals, Dhahran, Saudi Arabia

spin-lattice interactions as two energy reservoirs in the magnetic refrigerant (Szymczak *et al*., 2010). One of the significant properties of magnetic refrigerant that determines its suitability and usefulness for magnetic refrigeration is the Relative Cooling Power (RCP) (Zhang *et al*., 2011). RCP measures the amount or quantity of heat transferred between hot sinks and cold region in one ideal thermodynamic refrigeration cycle. Dependence of RCP of magnetic refrigerant and other magnetic properties on the structure of manganite-based material presents the opportunity of tuning the value of RCP to desired level through doping mechanism (Selmi *et al*., 2015a-c; Skini *et al*., 2014). However, experimental processes involved in the RCP tuning consume appreciable time and other valuable resources. This present research develops two-layer feedforward neural network model which is trained using Sensitivity-Based Linear Learning Method (SBLLM) to enhance learning speed and promote global convergence. The number of epoch and hidden neurons of the model was optimized using novel Gravitational Search Algorithm (GSA). The strengths and capacity of the developed GSA-SBLLM Model include ability to incorporate up to four different dopants into parent manganite-based material and estimates the value of its RCP at various concentration of the dopants, ability to estimate doping effect of a dopant on RCP of manganite-based material and ability to give quick and accurate estimation of RCP of manganite based materials.

Sensitivity-Based Linear Learning Method (SBLLM) is a technique of training two-layer feedforward neural network which gives characteristic fast learning speed to the network (Castillo *et al*., 2006). It implements linear training algorithm for each of the layers involved in the network. The basic operational principle of SBLLM is that it randomly assigns output to the first layer of the network and subsequently updates the outputs based on sensitivity formula until convergence is attained. This technique of training a network has the following merits, it saves computational time because it obtains local sensitivity of the least square errors with respect to the descriptors and target without extra computational cost, it has high learning speed and non-convergence to local minimum (Owolabi and Gondal, 2015; Olatunji *et al*., 2011, 2014). For the purpose of ensuring a Robust Model and improving the performance of the proposed method, the number of epoch and hidden neurons of SBLLM-based network were optimized using Gravitational Search Algorithm (GSA). GSA is a novel population based optimization algorithm that explores and exploits a search space purposely to converge at global minimum using Newtonian principle of gravity (Rashedi *et al*., 2009).

The Root Mean Square Error (RMSE), Mean Absolute Error (MAE) and Coefficient of Correlation (CC) which characterize the estimation accuracy of the proposed GSA-SBLLM Model for generalization to unseen data show that the developed model is precise and has excellent predictive capability. The obtained RMSE, MAE and CC for testing set of data are 29.69, 28.75 and 95.76%, respectively. The developed GSA-SBLLM Model was further utilized for estimating the RCP of various manganite-based materials and the obtained values agree well with the experimental results.

## MATERIALS AND METHODS

**Description of the proposed models:** The study presents the mathematical description of the proposed learning method. The description of the method used for ensuring optimum performance of the proposed model is also presented.

**Mathematical formulation of sensitivity based linear learning method of training neural network:** Consider a one-layer network that can be described by inputs-output relation presented in Eq. 1:

$$y_{j,\,d} = f_j \times \left( \sum_{i=0}^{|I|} w_{ji}\, x_{id} \right),\ j = \overline{1, |J|},\ d = \overline{1, |D|} \qquad (1)$$

Where:

I = The set of Inputs
J = The set of outputs
d = The set of data points
|.| = The number of elements in a set

Therefore, it is satisfied that $x_{0s} = 1$ and $w_{ji}$ represents the ith weighting coefficient for the jth neuron. Moreover, for the one-layer neural network, the sensitivities of the cost function Q (Castillo *et al*., 2006) with respect to the output and input data can be obtained as:

$$\frac{\partial Q}{\partial y_{pq}} = \frac{2\left( f_p^{-1}\left(y_{pq}\right) - \sum_{i=0}^{|I|} w_{pi} x_{iq} \right)}{f_p'\left(y_{pq}\right)},\ \forall p, q \qquad (2)$$

$$\frac{\partial Q}{\partial x_{pq}} = -2 \sum_{j=1}^{|J|} \left( f_j^{-1}\left(y_{jq}\right) - \sum_{i=0}^{|I|} w_{ji} x_{iq} \right) w_{jp},\ \forall p, q \qquad (3)$$

These sensitivity formulas are used for updating the initial output assigned to the first layer output and updated until convergence is achieved in two layer network. Considering a two-layer network as a composite of separate layers in which |K| represents the number of

hidden units and |D| denotes the number of data elements where, $x_{0d} = 1$, $z_{0d} = 1$, for each data sample dϵD, the cost function for both layers is presented in Eq. 4 and further simplified in Eq. 5 for a known intermediate output layer z:

$$Q(Z)=Q^{(1)}(Z)+Q^{(2)}(Z) \tag{4}$$

$$Q(z)=\sum_{d=1}^{|D|}\left(\sum_{k=1}^{|K|}\left(\sum_{i=0}^{|I|}w_{ki}^{(1)}x_{id}-f_k^{(1)^{-1}}(z_{kd})\right)^2+\sum_{j=1}^{|J|}\left(\sum_{k=0}^{|K|}w_{jk}^{(2)}z_{kd}-f_j^{(2)^{-1}}(y_{jd})\right)^2\right) \tag{5}$$

where the superscripts 1 and 2 are referring to the first and the second layer, respectively. Equation 6 and 7 show the sensitivity values with respect to the intermediate output $z_{kd}$ for two-layer network in accordance to Eq. 2 and 3 as described by Owolabi *et al*. (2017):

$$\frac{\partial Q}{\partial z_{kd}}=\frac{\partial Q^{(1)}}{\partial z_{kd}}+\frac{\partial Q^{(2)}}{\partial z_{kd}} \tag{6}$$

$$\frac{\partial Q}{\partial z_{kd}}=\frac{2\left(f_p^{-1}(z_{kd})-\sum_{i=0}^{|I|}w_{ki}^{(1)}x_{id}\right)}{f_p'(z_{kd})}-2\sum_{j=0}^{|J|}\left(f_j^{(2)^{-1}}(y_{jd})-\sum_{r=0}^{|K|}w_{jr}^{(2)}z_{rd}\right)w_{jk}^{(2)} \tag{7}$$

$$\text{for } k = 1, ..., |K| \text{ and } z_{os} = 1$$

for k = 1 and |K|. Finally, the intermediate output values z are approximated via. the Taylor series expansion as illustrated in Eq. 8:

$$Q(z+\Delta z)=Q(z)+\sum_{k=1}^{|K|}\sum_{d=1}^{|D|}\frac{\partial Q(z)}{\partial z_{kd}}\Delta z_{kd} \tag{8}$$

Where:

$$\Delta z=-\rho\frac{Q(z)}{\|\nabla Q\|^2}\nabla Q$$

ρ is relaxation factor.

**Description of gravitational search algorithm:** Gravitational Search Algorithm (GSA) represents a heuristic optimization algorithm which is based on the law of motion and the Newton's law of gravity (Rashedi *et al*., 2009). Exploitation step of the GSA is ensured by the slow movement of heavy objects which leads to good solutions. Four parameters which characterize every agent in GSA algorithm includes position, inertial mass, active gravitational mass and passive gravitational mass. The solution of the problem is given by the position of the mass while a fitness function is used to determine the gravitational and inertial masses (Owolabi *et al*., 2016; Goswami and Chakraborty, 2015; Niu *et al*., 2015; Ju and Hong, 2013; Rezaei and Nezamabadi-pour, 2015; Shuaib *et al*., 2015; Beigvand *et al*., 2016). In each iteration, the gravitational and inertia masses are adjusted where each mass determines a single solution. Since, all masses are attracted by masses which are heavier, the heaviest mass represents an optimum solution.

In GSA description, the positions of N agents are randomly initialized and are represented by points in s-dimensional space as illustrated by Eq. 9:

$$X_i=\left(x_i^1, ..., x_i^s\right), \forall i = 1, ..., N \tag{9}$$

where $x_i^s$ is the coordinate of the ith agent in the s-dimension. Then, the evolution of fitness is performed by computing the worst and the best fitness for each agent as well as the inertial Mass $M_{ai}$ using Eq. 10-13 coupled with fitness function:

$$b(it) = \min_{i=\overline{1,N}} fit_i(it) \tag{10}$$

$$w(it) = \max_{i=\overline{1,N}} fit_i(it) \tag{11}$$

$$m(it)=\frac{fit_i(it)-w(it)}{b(it)-w(it)} \tag{12}$$

$$M_i(t)=\frac{m_i(it)}{\sum_{i=1}^{N}m_i(it)} \tag{13}$$

where, the fitness values are given by $fit_i(it)$, for each $i=\overline{1,N}$ and b(it) represents the best fitness value at iteration it while w(it) is the worst fitness value, since, the problem addressed here is a minimization problem.

Suppose $F_{ij}^s(it)$ denotes the force influencing the ith agent due to jth agent at dimension s and ith iteration while $E_{ij}(it)$ represents the Euclidian distance between agents i and j, then the total Force $F_i^s(it)$ influencing the ith agent is computed using Eq. 14 coupled with Eq. 15 and 16 given that $G_0$ and α are predefined constants and T is the Total number of iterations:

$$F_i^s(t)=\sum_{j\in kbest,\, j\neq i}F_{i,j}^s(t) \tag{14}$$

$$F_{ij}^s(it)=G(it)\left(\frac{M_{pi}(it)\times M_{aj}(it)}{E_{ij}(it)+\varepsilon}\right)\left(x_j^s(it)-x_j^s(it)\right) \tag{15}$$

$$G(it) = G_0 \exp\left(-\frac{\alpha * it}{T}\right) \quad (16)$$

where, $K_{best}$ is the set of agents with best fitness values and biggest mass (the size of the set $K_{best}$ decreases by one in each iteration and at the end there will be only one agent) and ε is a predefined constant.

Using the assumption contained in Eq. 17 where $M_{ai}$, $M_{pi}$, $M_{ii}$ represent the active gravitational Mass, passive gravitational Mass and inertia Mass, respectively the acceleration of the agent i is computed using Eq. 18:

$$M_{ai} = M_{pi} = M_{ii}, i = \overline{1,N} \quad (17)$$

$$a_i^s(it) = \frac{F_i^s(it)}{M_{ii}(it)} \quad (18)$$

The velocities and positions of the agents at the iteration t+1 are evaluated and updated using Eq. 19 and 20:

$$v_i^s(it+1) = rand_i\left(xv_i^s(it) + a_i^s(it)\right) \quad (19)$$

$$x_i^s(it+1) = x_i^s(it) + v_i^s(it+1) \quad (20)$$

The procedures are repeated until the specified maximum iteration is reached.

**Development of GSA-SBLLM Model:** The description of the dataset used for developing the proposed GSA-SBLLM Model is presented in this study. The computational methodology adopted while developing GSA-SBLLM Model is also detailed in this study.

**Dataset description:** The dataset used for developing the proposed GSA-SBLLM Model consists of fifty experimental values of relative cooling power coupled with the ionic radii as well as the concentration of each element present in desired manganite based materials. The experimental values of RCP for model validation are obtained from the literature (Selmi *et al*., 2015a-c; Cherif *et al*., 2014; Mleiki *et al*., 2015; Kossi *et al*., 2015; Oumezzine *et al*., 2014; Mahjoub *et al*., 2014; Ghodhbane *et al*., 2014; Wang and Jiang, 2013). For manganite based material with general chemical formula given in Eq. 21 where R and A, respectively represent rare earth cation, alkali metal or alkaline earth cation while C and D can be any other periodic metals such as transition metals among others, the ionic radii of cations in Eq. 21 and their respective concentrations serve as the inputs to the proposed GSA-SBLLM Model. The proposed GSA-SBLLM Model can incorporate up to four dopants to manganite so as to widen the applicability of the model while zero value is assigned to the ionic radius or concentration of a cation that does not present in manganite based material of interest:

$$R_{1-x-y}A_xC_yMn_{1-z}D_zO_3 \quad (21)$$

The descriptors to the proposed model and experimental RCP are contained in Table 1. The table also shows the outcomes of the statistical analysis performed on the dataset. Among the useful information that can be obtained from mean, range and standard deviation of the dataset as illustrated in the table is the consistency of the data-points and a measure of how they are far apart. Correlations between each descriptor and the target are also presented. The correlation measures the extent of linear relationship that exists between a descriptor and target and ranges from 0-1 with 0 showing absence of linear relationship while 1 indicates perfect linear relationship. The results presented in Table 1 are in percentage where some descriptors are positively correlated with the RCP while others are negatively correlated. The choice of the proposed model in this work is to effectively capture the non-linear relationship between the descriptors and the target, since, they are weakly connected in terms of linear relationship and linear modeling technique would perform poorly in this regards.

**Computational description of GSA-SBLLM Model:** The following computational procedures and steps were adopted while developing GSA-SBLLM hybrid intelligent model for estimating RCP of manganite.

**Step 1:** Dataset randomization and partitioning: the fifty data-points available for simulation were randomized and

Table 1: Results of the statistical analysis

| Variables | R | Con.R | A | Con.A | C | Con.C | D | Con.D | RCP |
|---|---|---|---|---|---|---|---|---|---|
| Mean (J/K) | 115.35 | 0.6754 | 119.74 | 0.24 | 37.02 | 0.08 | 38.04 | 0.04 | 157.09 |
| Maximum (J/K) | 117.20 | 0.9500 | 149.00 | 0.40 | 149.00 | 0.45 | 100.00 | 0.30 | 405.72 |
| Minimum (J/K) | 109.80 | 0.1500 | 113.00 | 0.01 | 0.00 | 0.00 | 0.00 | 0.00 | 9.72 |
| Standard deviation (J/K) | 002.52 | 0.1400 | 9.60 | 0.09 | 60.24 | 0.15 | 45.27 | 0.06 | 118.01 |
| Correlation coefficient (%) | -65.49 | -29.4400 | -36.87 | 5.25 | 33.82 | 26.88 | 48.40 | 25.21 | |

separated into training and testing portions in the ratio of 80-20, respectively. This step is necessary for ensuring even distribution of data-points and efficient as well as reproducible computations. The partitioned data-points were used for the rest of the modeling task.

**Step 2:** Initialization of GSA agents. The positions $X_i=(x_i^1,...,x_i^s)$ of N agents are initialized. Each agent encodes the number of epoch and hidden neuron for training two-layer network using SBLLM.

**Step 3:** The descriptors in the training dataset (ionic radii and the corresponding concentrations) were fed into two-layer feedforward neural network with randomly assigned intermediate RCP values. The intermediate outputs (RCP) are updated using sensitivities formulas coupled with experimental values of RCP in the training dataset until convergence is achieved for each of the initialized agents, thereby the weights in each of the layer are learnt and the fitness (root mean square error between the estimated and experimental RCP) of each of the agent are computed.

**Step 4:** Inertial mass of the agents are calculated based on the fitness and the gravitational pull $\left(F_i^s(t)=\sum_{j\in Kbest,j\neq i}F_{ij}^s(t)\right)$ on each of the agents are also evaluated.

**Step 5:** The position and velocity of the agents are updated. The procedures (Step 3 and 4) are repeated until maximum iteration is reached.

**Step 6:** The optimum position of the most sluggish (this encodes the number of epoch and hidden neurons) agent, learnt weights and the descriptors in the testing dataset are used in estimating RCP and the obtained values are compared with the experimental values.

## RESULTS AND DISCUSSION

This study presents the results of the developed GSA-SBLLM Model. The comparison between the results of the developed model and the experimentally measured RCP is also presented. The influence of several dopants on many classes of manganite is investigated and presented in this study.

**Influence of optimum GSA parameters on the performance of GSA-SBLLM Model:** Parameters that influence the performance of GSA include the initial population of agents and gravitational constant while the optimum gravitational constant can be controlled by adjusting the initial value of gravitational constant and the parameter alpha that controls the rate of gravitational

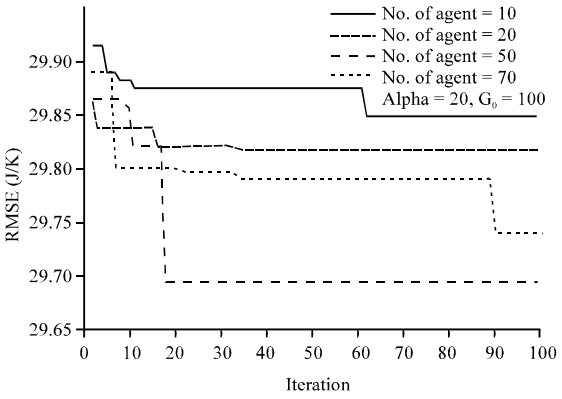


Fig. 1: Dependence of model performance on the initial population of the agents

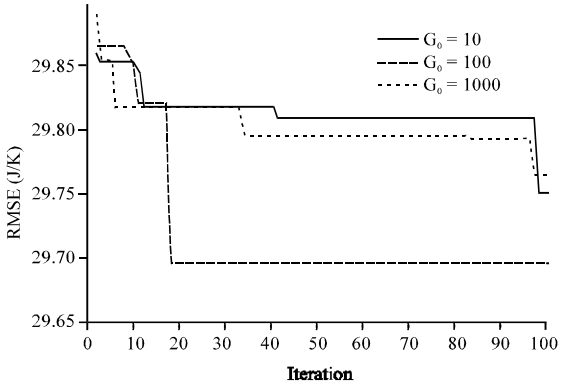


Fig. 2: Performance sensitivity of the model to gravitational pull

decay. The exploration capacity of the algorithm becomes lower for small initial population of the agents while complexity and inadequate exploitation occur in case of large number of agents assessing the global solution. Similarly, agents experience strong gravitational pull which affect both exploration and exploitation ability at a large value of initial gravitational constant while the weak gravitational pull also affect the performance of the algorithm. Figure 1 shows the influence of initial population of agents on the model performance. For 10 and 20 number of agents, weaker exploration was observed and optimum exploration was obtained at 50 numbers of agents. When the number of agents exceeds this threshold, inadequate exploitation set in and the model was trapped in local minimum. Similarly, the effect of gravitational pull on the performance of GSA-SBLLM is shown in Fig. 2. Above the initial value of 100, GSA-SBLLM converged at local minimum. The optimum values of GSA-SBLLM Model are presented in Table 2.

Table 2: Optimum GSA-SBLLM parameters

| Model parameters | Optimum values |
|---|---|
| Number of epoch | 4468 |
| Hidden neuron | 67 |
| Initial population of agents | 50 |
| Initial value of gravitational constant | 100 |
| Alpha | 20 |
| Maximum iteration | 100 |

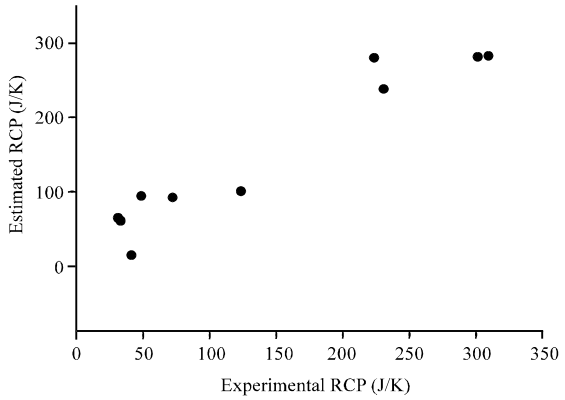


Fig. 3: Correlation cross-plot between estimated and experimentally measured RCP (cc = 95.76%)

**Measures of generalization and prediction ability of the developed GSA-SBLLM Model:** The estimation accuracy of the developed GSA-SBLLM Model was evaluated using Correlation Coefficient (CC), Root Mean Square Error (RMSE) and Mean Absolute Error (MAE) for both training and testing set of data. The correlation cross-plot between the estimated RCP and measured values for testing dataset is presented in Fig. 3.

High degree of correlation was obtained between RCP estimated using GSA-SBLLM Model and the experimentally measured values. This translates to excellent prediction ability of the proposed model. The values of RMSE and MAE for both training and testing dataset are also presented in Table 3. The model shows higher improvement as measured through lower RMSE, lower MAE and higher CC during testing stage. This shows the excellent predictive strength of the developed GSA-SBLLM Model. Hence, the model can be used for determining RCP of various kinds of manganite-based materials for magnetic refrigeration performance enhancement.

**Doping effect of Praseodymium (Pr) on RCP of $Sm_{0.35}Pr_XSr_{0.45}MnO_3$ manganite:** In order to further assess the robustness of the developed GSA-SBLLM Model it is deployed for investigating the influence of Praseodymium (Pr) doping on RCP of $Sm_{0.35}Pr_XSr_{0.45}MnO_3$ manganite and the results of the model are illustrated in Fig. 4. In this investigation, only the descriptors were

Table 3: Measures of estimation accuracy of GSA-SBLLM Model

| Performance measure parameter | Training dataset | Testing dataset |
|---|---|---|
| Correlation coefficient (%) | 84.06 | 95.76 |
| Root mean square error (J/K) | 64.31 | 29.69 |
| Mean absolute error (J/K) | 39.65 | 28.75 |

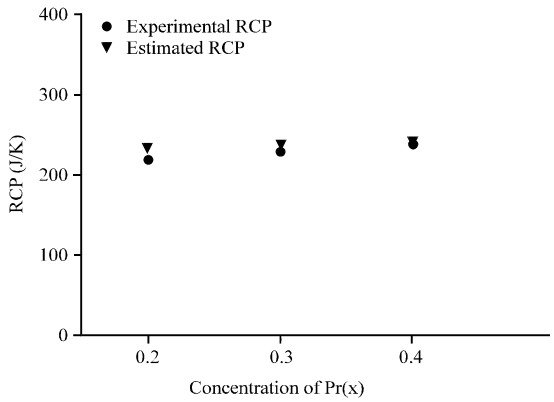


Fig. 4: Effact of Pr-doping on RCP of $Sm_{0.35}Pr{\times}Sr_{0.45}MnO_3$

supplied into the model and the model estimates RCP of the material using its acquired pattern during the training phase. Pr-doping slightly raises RCP of $Sm_{0.35}Pr_XSr_{0.45}MnO_3$ material as shown in Fig. 4. Figure 4 also shows excellent agreement between measured and estimated values of RCP. Increase in RCP value due to $Pr^{3+}$ ion substitution for $Sm^{3+}$ can be attributed to $MnO_6$ octahedra distortion created by $Pr^{3+}$ ions as a result of its higher ionic radius as compared to $Sm^{3+}$ ions. This increases Mn-O-Mn interaction and widens bandwidth that promotes parallel alignment of $Mn^{3+}/Mn^{4+}$ spins to magnetic field.

**Doping effect of Titanium (Ti) on RCP of $La_{0.7}Sr_{0.25}Na_{0.05}Mn_{1-x}Ti_XO_3$ manganite:** The effect of Titanium (Ti) doping on RCP of $La_{0.7}Sr_{0.25}Na_{0.05}Mn_{1-x}Ti_XO_3$ manganite-based material was also investigated and presented in Fig. 5. The outcomes of the simulation show that titanium lowers the RCP values of $La_{0.7}Sr_{0.25}Na_{0.05}Mn_{1-x}Ti_XO_3$ as shown in the Fig. 5. Results of GSA-SBLLM Model also agree well with the experimentally measured values (Kossi *et al*., 2015). This shows excellent estimation and generalization capacity of the developed model. Reduction in the value of RCP due to titanium substitution can be attributed to the reduction in the maximum entropy change which is consequent upon non-magnetic nature of the dopant (Nisha *et al*., 2013; Phan *et al*., 2005, 2010). Titanium enhances super-exchange interaction ($Mn^{+4}$-$O^{-2}$-$Mn^{+4}$) and lowers $Mn^{+4}$ content (which consequently decrease the double exchange ferromagnetic interactions) as a results of change in $Mn^{+3}/Mn^{+4}$ ratio as well as reduction in the number of hopping sites (Koubaa *et al*., 2011).

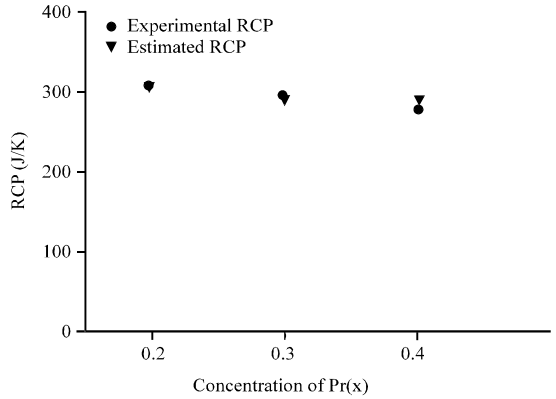


Fig. 5: Effect of Ti-doping on RCP of $La_{0.7}Na_{0.05}Mn_{1-X}Ti_xO_3$ manganite based material

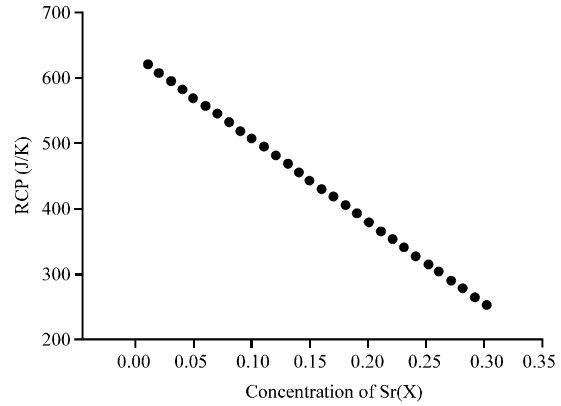


Fig. 6: Effect of Sr doping on RCP of $Pr_{0.6}$ $Ca_{1-X}$ $Sr_X$ $Mn_{0.925}$ $Fe_{0.075}$ $O_3$

**Doping effect of Strontium (Sr) on RCP of $Pr_{0.6}Ca_{1-X}Sr_XMn_{0.925}Fe_{0.075}O_3$ manganite:** After establishing the excellent estimation and generalization capacity of GSA-SBLLM Model through validation of its estimates with the experimentally measured RCP, the developed GSA-SBLLM was employed for determining the effect of strontium doping on RCP of $Pr_{0.6}Ca_{1-X}Sr_XMn_{0.925}Fe_{0.075}O_3$ manganite and the results of the simulation is presented in Fig. 6. The results show that incorporation of strontium dopants into crystal structure of $Pr_{0.6}Ca_{1-X}Sr_XMn_{0.925}Fe_{0.075}O_3$ lowers its RCP values. The value of RCP decreases as the concentration of strontium increases as presented in Fig. 6. This is expected since the substituted $Sr^{+2}$ ions are of larger ionic radius as compared to $Ca^{2+}$ and consequently creates $MnO_6$ octahedra distortion.

**Doping effect of alkali metals on RCP of $La_{0.7}Sr_{0.25}X_{0.05}Mn_{0.9}Ti_{0.1}O_3$ manganite:** Influence of alkali metals substitution on RCP value of $La_{0.7}Sr_{0.25}X_{0.05}$ $Mn_{0.9}Ti_{0.1}O_3$ material using the developed GSA-SBLLM Model is presented in Fig. 7. The results of modeling and simulation show that the RCP of the material increases as the number of ionic radii of the metal increases with Lithium (Li) having lower RCP while Cesium (Cs) gives highest RCP value.

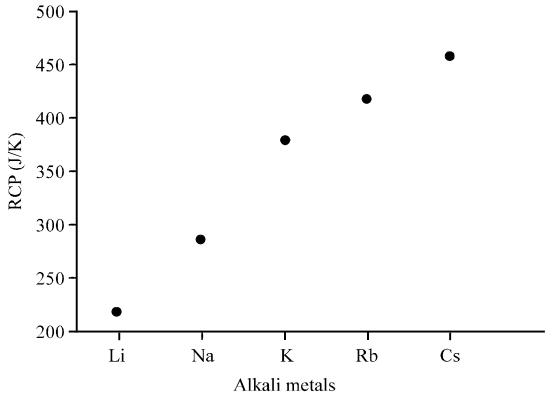


Fig. 7: Effect of alkali metal doping on RCP of $La_{0.7}$ $Sr_{0.25}$ $X_{0.05}$ $Mn_{0.9}$ $Ti_{0.1}$ $O_3$ Manganite based material

## CONCLUSION

GSA-SBLLM Model was developed for determining RCP of doped manganite using ionic radii and the concentration of the dopants as the descriptors. The influence of the initial population of agents as well as the gravitational pull on predictive capacity of the model was simulated and discussed. The generalization strength of the proposed GSA-SBLLM Model was assessed using correlation coefficient, mean absolute error and root mean square error between the model estimates and the measured values. Low value of root mean square error and high value of correlation coefficient characterize the developed GSA-SBLLM Model. The developed model was implemented in estimating the; doping effect of praseodymium on $Sm_{0.35}Pr_XSr_{0.45}MnO_3$, effect of titanium on RCP of $La_{0.7}Sr_{0.25}Na_{0.05}Mn_{1-x}Ti_XO_3$, effect of strontium on RCP of $Pr_{0.6}Ca_{1-X}Sr_XMn_{0.925}Fe_{0.075}O_3$ and influence of alkali metals on RCP of $La_{0.7}Sr_{0.25}X_{0.05}Mn_{0.9}Ti_{0.1}O_3$ manganite-based materials and the estimated RCP values show excellent agreement with the measured values. With the aid of the developed model, the RCP of manganite-based materials can be easily determined for enhanced magnetic system of refrigeration.

## ACKNOWLEDGEMENT

The support received from University of Dammam and King Fahd University of Petroleum and Minerals is acknowledged.

## REFERENCES


Beigvand, S.D., H. Abdi and M.L. Scala, 2016. Combined heat and power economic dispatch problem using gravitational search algorithm. Electr. Power Syst. Res., 133: 160-172.

Bettaibi, A., R. M'nassri, A. Selmi, H. Rahmouni and N. Chniba-Boudjada *et al*., 2015. Effect of chromium concentration on the structural, magnetic and electrical properties of praseodymium-calcium manganite. J. Alloys Compd., 650: 268-276.

Bruck, E., 2005. Developments in magnetocaloric refrigeration. J. Phys. D. Appl. Phys., 38: R381-R391.

Castillo, E., B. Guijarro-Berdinas, O. Fontenla-Romero and A. Alonso-Betanzos, 2006. A very fast learning method for neural networks based on sensitivity analysis. J. Mach. Learn. Res., 7: 1159-1182.

Cherif, R., E.K. Hlil, M. Ellouze, F. Elhalouani and S. Obbade, 2014. Magnetic and magnetocaloric properties of $La_{0.6}Pr_{0.1}Sr_{0.3}Mn_{1-x}Fe_xO_3$ (0 = x = 0.3) manganites. J. Solid State Chem., 215: 271-276.

Gdaiem, M.A., S. Ghodhbane, A. Dhahri, J. Dhahri and E.K. Hlil, 2016. Effect of cobalt on structural, magnetic and magnetocaloric properties of $La_{0.8}Ba_{0.1}Ca_{0.1}Mn_{1-x}Co_xO_3$ (x= 0.00, 0.05 and 0.10) manganites. J. Alloys Compd., 681: 547-554.

Ghodhbane, S., E. Tka, J. Dhahri and E.K. Hlil, 2014. A large magnetic entropy change near room temperature in $La_{0.8}$, $Ba_{0.1}$, $CaM_{0.1}$, $Mn_{0.97}$ $Fe_{0.03}O_3$ perovskite. J. Alloys Compd., 600: 172-177.

Goswami, D. and S. Chakraborty, 2015. Parametric optimization of ultrasonic machining process using gravitational search and fireworks algorithms. Ain Shams Eng. J., 6: 315-331.

Gschneidner Jr, K.A., V.K. Pecharsky and A.O. Tsokol, 2005. Recent developments in magnetocaloric materials. Rep. Prog. Phys., 68: 1479-1539.

Kossi, S.E., S. Ghodhbane, S. Mnefgui, J. Dhahri and E.K. Hlil, 2015. The impact of disorder on magnetocaloric properties in Ti-doped manganites of $La_{0.7}Sr_{0.25}Na_{0.05}Mn_{(1-x)}TixO_3$ (0= x= 0.2). J. Magn. Magn. Mater., 395: 134-142.

Koubaa, M., Y. Regaieg, W.C. Koubaa, A. Cheikhrouhou and S. Ammar-Merah *et al*., 2011. Magnetic and magnetocaloric properties of lanthanum manganites with monovalent elements doping at A-site. J. Magn. Magn. Mater., 323: 252-257.

Mahjoub, S., M. Baazaoui, R. M'nassri, H. Rahmouni and N.C. Boudjada *et al*., 2014. Effect of Iron substitution on the structural, magnetic and magnetocaloric properties of $Pr_{0.6}Ca_{0.1}Sr_{0.3}Mn_{1-x}FexO_3$ (0-x-0.075) manganites. J. Alloys Compd., 608: 191-196.

Messaoui, I., M. Kumaresavanji, K. Riahi, W.C. Koubaa and M. Koubaa *et al*., 2017. Magnetic, magnetocaloric and critical behavior study of La0. 78Pb0. 22MnO3 manganite near room-temperature. Ceram. Intl., 43: 498-506.

Mleiki, A., S. Othmani, W. Cheikhrouhou-Koubaa, M. Koubaa and A. Cheikhrouhou *et al*., 2015. Effect of praseodymium doping on the structural, magnetic and magnetocaloric properties of $Sm_{0.55-x}Pr_xSr_{0.45}MnO_3$ (0.1=x=0.4) manganites. J. Alloys Compd., 645: 559-565.

Nisha, P., S.S. Pillai, M.R. Varma and K.G. Suresh, 2013. Influence of cobalt on the structural, magnetic and magnetocaloric properties of $La_{0.67}Ca_{0.33}MnO_3$. J. Magn. Magn. Mater., 327: 189-195.

Niu, P., C. Liu, P. Li and G. Li, 2015. Optimized support vector regression model by improved gravitational search algorithm for flatness pattern recognition. Neural Comp. Appl., 26: 1167-1177.

Olatunji, S.O., A. Selamat and A.A.A. Raheem, 2011. An hybrid model through the fusion of sensitivity based linear learning method and type-2 fuzzy logic systems for modeling PVT properties of crude oil systems. Proceedings of the 2011 5th Malaysian Conference on Software Engineering (MySEC), December 13-14, 2011, IEEE, Johor Bahru, Malaysia, ISBN: 978-1-4577-1530-3, pp: 354-360.

Olatunji, S.O., A. Selamat and A.A.A. Raheem, 2014. Improved sensitivity based linear learning method for permeability prediction of carbonate reservoir using interval type-2 fuzzy logic system. Appl. Soft Comp., 14: 144-155.

Oumezzine, E., S. Hcini, E.K. Hlil, E. Dhahri and M. Oumezzine, 2014. Effect of Ni-doping on structural, magnetic and magnetocaloric properties of $La_{0.6}Pr_{0.1}Ba_{0.3}Mn_{1-x}NixO_3$ nanocrystalline manganites synthesized by Pechini sol-gel method. J. Alloys Compd., 615: 553-560.

Owolabi, T.O. and M.A. Gondal, 2015. Estimation of surface tension of methyl esters biodiesels using computational intelligence technique. Appl. Soft Comp., 37: 227-233.

Owolabi, T.O., K.O. Akande, S.O. Olatunji, A. Alqahtani and N. Aldhafferi, 2016. Estimation of curie temperature of manganite-based materials for magnetic refrigeration application using hybrid gravitational based support vector regression. AIP. Adv., 6: 105009-1-105009-12.

Owolabi, T.O., K.O. Akande, S.O. Olatunji, A. Alqahtani and N. Aldhafferi, 2017. Incorporation of GSA in SBLLM-based neural network for enhanced estimation of magnetic ordering temperature of manganite. J. Intell. Fuzzy Syst., 33: 1225-1233.

Phan, M.H., S.C. Yu and N.H. Hur, 2005. Excellent magnetocaloric properties of $La_{0.7}Ca_{0.3-x}Sr_xMnO_3$ (0.05=x=0.25) single crystals. Appl. Phys. Lett., 86: 072504-1-072504-3.

Phan, M.H., V. Franco, N.S. Bingham, H. Srikanth, N.H. Hur and S.C. Yu, 2010. Tricritical point and critical exponents of La0.7Ca0.3-xSrxMnO3 (x = 0, 0.05, 0.1, 0.2, 0.25) single crystals. J. Alloys Compounds, 508: 238-244.

Rashedi, E., H. Nezamabadi-Pour and S. Saryazdi, 2009. GSA: A gravitational search algorithm. Inform. Sci., 179: 2232-2248.

Rezaei, M. and H. Nezamabadi-Pour, 2015. Using gravitational search algorithm in prototype generation for nearest neighbor classification. Neurocomputing, 157: 256-263.

Selmi, A., R. M'nassri, W. Cheikhrouhou-Koubaa, N.C. Boudjada and A. Cheikhrouhou, 2015a. Effects of partial Mn-substitution on magnetic and magnetocaloric properties in $Pr_{0.7}Ca_{0.3}Mn_{0.95}X_{0.05}O_3$ (Cr, Ni, Co and Fe) manganites. J. Alloys Compd., 619: 627-633.

Selmi, A., R. M'nassri, W. Cheikhrouhou-Koubaa, N.C. Boudjada and A. Cheikhrouhou, 2015b. The effect of Co doping on the magnetic and magnetocaloric properties of $Pr_{0.7}Ca_{0.3}Mn_{1-x}Co_xO_3$ manganites. Ceram. Intl., 41: 7723-7728.

Selmi, A., R. M'nassri, W. Cheikhrouhou-Koubaa, N.C. Boudjada and A. Cheikhrouhou, 2015c. Influence of transition metal doping (Fe, Co, Ni and Cr) on magnetic and magnetocaloric properties of $Pr_{0.7}Ca_{0.3}MnO_3$ manganites. Ceram. Intl., 41: 10177-10184.

Shuaib, Y.M., M.S. Kalavathi and C.C.A. Rajan, 2015. Optimal capacitor placement in radial distribution system using gravitational search algorithm. Intl. J. Electr. Power Energy Syst., 64: 384-397.

Skini, R., A. Omri, M. Khlifi, E. Dhahri and E.K. Hlil, 2014. Large magnetocaloric effect in lanthanum-deficiency manganites $La_{0.8-x-x}Ca_{0.2}MnO_3$ (0.00 = x = 0.20) with a first-order magnetic phase transition. J. Magn. Magn. Mater., 364: 5-10.

Szymczak, R., R. Kolano, A. Kolano-Burian, V.P. Dyakonov and H. Szymczak, 2010. Giant magnetocaloric effect in manganites. Acta Phys. Polon. A., 117: 203-206.

Taran, S., C.P. Sun, C.L. Huang, H.D. Yang and A.K. Nigam *et al*., 2015. Electrical and magnetic properties of Y-doped $La_{0.5}$ $Sr_{0.5}$ $MnO_3$ manganite system: Observation of step-like magnetization. J. Alloys Compd., 644: 363-370.

Wang, Z. and J. Jiang, 2013. Magnetic entropy change in perovskite manganites $La_{0.7}A_{0.3}MnO_3La_{0.7}A_{0.3}Mn_{0.9}Cr_{0.1}O_3$ (A = Sr, Ba, Pb) and Banerjee criteria on phase transition. Solid State Sci., 18: 36-41.

Zhang, Q., S. Thota, F. Guillou, P. Padhan and V. Hardy *et al*., 2011. Magnetocaloric effect and improved relative cooling power in ($La_{0.7}Sr_{0.3}MnO_3$/$SrRuO_3$) superlattices. J. Phys. Condensed Matter, 23: 1-6.